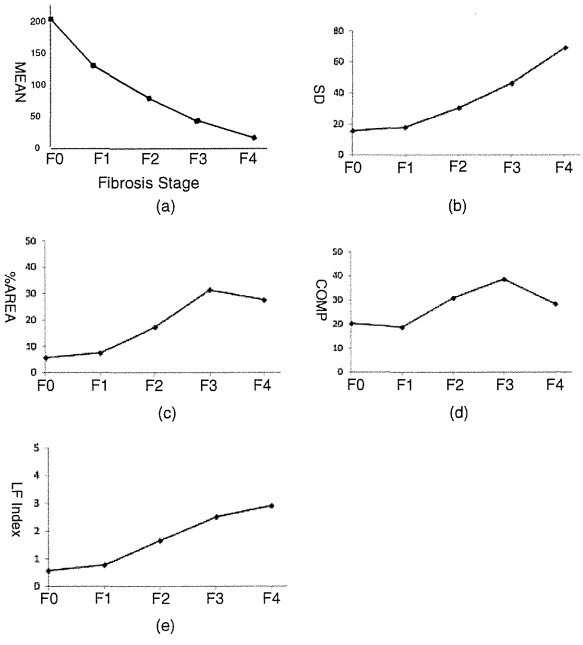

Fig. 10. Features of strain image and LF index as a function of fibrosis stage in the case of $n = 2$, and $\alpha = \beta = 0.1$ [parameters in eqs. (6) and (7)]: (a) MEAN, (b) SD, (c) %AREA, (d) COMP, and (e) LF index.

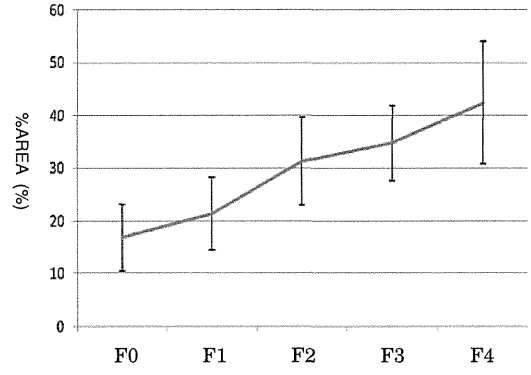

Fig. 11. Change in %AREA as a function of fibrosis stage (clinical data analysis).

simulation analysis is for a single case, the LF index obtained using a mechanical model of fibrosis progression coincides with the result of the clinical data analysis.

These results indicate that even in diffuse diseases like chronic hepatitis, the pattern of strain images is related to the fibrous structure changes caused by hepatic disease and can be used to derive features for quantitative evaluation of fibrosis stage.

On the other hand, there remain several problems to be solved for the development of a clinically useful method. For example, the parameters of models described in §2.2.1 and §2.2.2 are defined only to determine the size of the nodules or the rate of stiffness increase. Therefore, they do not directly indicate the physical characteristic of the liver. In particular, the number of iterations is an important parameter, although there is no *a priori* information at present. In terms of the parameter n, representing the rate of stiffness increase, if parameters are set to $n = 2$ and $\alpha = \beta = 0.1$, the staging is accelerated, as shown in Fig. 10. To tune or optimize these parameters, it is indispensable to continue the simulation under several conditions and compare the results with a large number of clinical data.

As mentioned in §2.1, chronic hepatitis is scored by fibrosis staging and grading. Our clinical research validates that the LF index obtained by RTE stably reflects the fibrosis stage without being influenced by variables of inflammatory state or blood pressure. On the other hand, it is reported that the values measured by FibroScan® are influenced by variables such as hepatic steatosis and flares of transaminases.[21,22] This indicates that shear wave velocity is also changed by factors other than fibrosis stage. In terms of shear wave velocity measurement, some methods using acoustic radiation force for shear wave generation within the body have been recently developed such as acoustic radiation force impulse (ARFI) imaging[29] and shear wave elastography (SWE).[30] These methods can also be used as noninvasive methods of assessing tissue stiffness. In addition, it is expected to utilize different diagnosis information by using both methods, that is, strain image and shear wave image.

4. Conclusions

In this study, we proposed a mechanical model of fibrosis progression. From the strain distribution, we could see that the area of low strain increases, and the strain distribution becomes increasingly complex as fibrosis progresses. The extracted features of strain and derived the LF liver index showed a definite correlation with fibrosis progression and coincided with the result of clinical data analysis. This indicates that even in diffuse diseases like chronic hepatitis, the pattern of strain images is related to the fibrous structure changes caused by hepatic disease and can be used to derive features for quantitative evaluation of fibrosis stage.

As mentioned above, to optimize the parameters used for simulation analysis, it is indispensable to continue the simulation under several conditions and compare the results with a large number of clinical data. For example, although the number of iterations for the conjugating process does not directly indicate the physical characteristic of the liver, the %AREA may be a useful reference to relate the number of iterations to the fibrosis stages. Figure 11 shows the %AREA obtained by clinical data analysis, which increases as a function of fibrosis stage and is similar to Fig. 9(c).

In addition, for future work, there remain some problems to be investigated. To extract reliable diagnosis information from a strain image, a stable data acquisition system that is robust against noise and artifacts must be developed. To improve the precision of simulation, we must investigate a way to obtain the precise values of Young's modulus for each component, such as the parenchyma and fibrous portion, for example, by microscopic measurement of tissues for each stage of hepatitis. Finally, in terms of the extraction of image features, it is one of the most important themes of this research to extract more appropriate features to be useful for the precise diagnosis of chronic hepatitis.

1) A. Ohshima: Proc. 123rd Symp. Japanese Association of Medical Sciences, 2003, p. 13 [in Japanese].
2) National Institutes of Health Consensus Development Conference Statement. Management of Hepatitis C: Hepatology **36** (2002) S3.
3) A. A. Bravo, S. G. Sheth, and S. Chopra: New Engl. J. Med. **344** (2001) 495.
4) I. Sporea, A. Popescu, and R. Sirli: World J. Gastroenterol. **14** (2008) 3396.
5) P. Bedossa, D. Dargère, and V. Paradis: Hepatology **38** (2003) 1449.
6) M. Ziol, A. Handra-Luca, A. Kettaneh, C. Christidis, F. Mal, F. Kazemi, V. de Ledinghen, V. P. Marcelin, D. Dhumeaux, J. C. Trinchet, and M. Beaugran: Hepatology **41** (2005) 48.
7) U. Arena, F. Vizzutti, G. Corti, S. Ambu, C. Stasi, S. Bresci, S. Moscarella, V. Boddi, A. Petrarca, G. Laffi, F. Marra, and M. Pinzani: Hepatology **47** (2008) 380.
8) Y. Fujii, N. Taniguchi, and K. Itho: Med. Imaging Technol. **21** (2003) 117.
9) T. Nishimura, H. Watanabe, M. Ito, Y. Matsuoka, K. Yano, M. Daikoku, H. Yaysuhasshi, K. Dohmen, and H. Ishibashi: Br. J. Radiol. **78** (2005) 189.
10) T. Yamaguchi, H. Hachiya, K. Kato, H. Fukuda, and M. Ebara: Jpn. J. Appl. Phys. **39** (2000) 3266.
11) T. Yamaguchi, K. Nakamura, and H. Hachiya: Jpn. J. Appl. Phys. **42** (2003) 3292.
12) Y. Igarashi, H. Ezuka, T. Yamaguchi, and H. Hachiya: Jpn. J. Appl. Phys. **49** (2010) 07HF06.
13) T. Shiina, N. Nitta, E. Ueno, and J. C. Bamber: J. Med. Ultrason. **29** (2002) 119.
14) M. Yamakawa, N. Nitta, T. Shiina, M. Matsumura, S. Tamano, T. Mitake, and E. Ueno: Jpn. J. Appl. Phys. **42** (2003) 3265.
15) A. Itoh, E. Ueno, E. Tohno, H. Kamma, H. Takahashi, T. Shiina, M. Yamakawa, and T. Matsumura: Radiology **231** (2006) 341.
16) K. Fujimoto, M. Kato, A. Tonomura, N. Yada, C. Tatsumi, M. Oshita, S. Wada, K. Ueshima, T. Ishida, T. Furuta, M. Yamasaki, M. Tsujimoto, M. Motoki, T. Mitake, S. Kim, K. Yamamoto, T. Shiina, M. Kudo, and N. Hayashi: Kanzo **51** (2010) 539 [in Japanese].
17) A. Tonomura, M. Motoki, T. Mitake, K. Fujimoto, M. Kato, C. Tatsumi, N. Yada, K. Ueshima, M. Kudo, and T. Shiina: Proc. 22nd Kanto-section Meet. JSUM, 2010, p. 36 [in Japanese].
18) C. Tatsumi, M. Kudo, K. Ueshima, S. Kitai, E. Ishikawa, N. Yada, S. Hagiwara, T. Inoue, Y. Minami, H. Chung, K. Maekawa, K. Fujimoto, M. Kato, A. Tonomura, T. Mitake, and T. Shiina: Intervirology **53** (2010) 76.
19) F. Ichida, T. Tsuji, M. Omata, T. Ichida, K. Inoue, T. Kaminuma, G. Yamada, K. Hino, O. Yokosuka, and H. Suzuki: Int. Hepatol. Commun. **36** (1996) 112.
20) L. Sandrin, B. Fourquet, J. M. Hasquenoph, S. Yon, C. Fournier, F. Mal, C. Christidis, M. Ziol, B. Poulet, F. Kazemi, M. Beaugrand, and R. Palau: Ultrasound Med. Biol. **29** (2003) 1705.
21) M. Friedrich-Rust, M. F. Ong, S. Martens, C. Sarrazin, J. Bojunga, S. Zeuzem, and E. Herrmann: Gastroenterology **134** (2008) 960.
22) U. Arena, F. Vizzutti, G. Corti, S. Ambu, C. Stasi, S. Bresci, S. Moscarella, V. Boddi, A. Petrarca, G. Laffi, F. Marra, and M. Ponzani: Hepatology **47** (2008) 380.
23) T. Shiina, M. M. Doyley, and J. C. Bamber: Proc. IEEE Ultrasonics Symp., 1996, 1331.
24) M. Yamakawa and T. Shiina: Jpn. J. Appl. Phys. **40** (2001) 3872.
25) E. Tohno and E. Ueno: Breast Cancer **15** (2008) 200.
26) National Center for Global Health and Medicine, Disease Control and Prevention Center (2008) [http://www.ncgm.go.jp/center/formedsp_cir.html] [in Japanese].
27) T. Yasuda, T. Takeda, Y. Nakayama, K. Uehata, H. Sakaguchi, M. Seki, A. Sawada, M. Yamashita, K. Abo, S. Takeda, and H. Asai: presented at 151st Osaka Abdomen Ultrasound, 2005 [in Japanese].
28) M. Ziol, A. Handra-Luca, A. Kettaneh, C. Christidis, F. Mal, F. Kazemi, V. de Lédinghen, P. Marcellin, D. Dhumeaux, J. C. Trinchet, and M. Beaugrand: Hepatology **41** (2005) 48.
29) M. L. Palmeri, M. H. Wang, J. J. Dahl, K. D. Frinkley, and K. R. Nightingale: Ultrasound Med. Biol. **34** (2008) 546.
30) J. Bercoff, M. Tanter, and M. Fink: IEEE Trans. Ultrason. Ferroelectr. Freq. Control **51** (2004) 396.

Oncology

Oncology 2013;84(suppl 1):3–12
DOI: 10.1159/000345883

Published online: February 20, 2013

Novel Image Analysis Method Using Ultrasound Elastography for Noninvasive Evaluation of Hepatic Fibrosis in Patients with Chronic Hepatitis C

Kenji Fujimoto[a, b] Michio Kato[b] Masatoshi Kudo[c] Norihisa Yada[c] Tsuyoshi Shiina[d] Kazuomi Ueshima[c] Yukinori Yamada[e] Tetsushi Ishida[f] Masayoshi Azuma[f] Masaru Yamasaki[g] Keiji Yamamoto[b] Norio Hayashi[h] Tetsuo Takehara[i]

[a]Division of Clinical Research and [b]Department of Internal Medicine, National Hospital Organization Minamiwakayama Medical Center, Tanabe, [c]Department of Gastroenterology and Hepatology, Kinki University School of Medicine, Osakasayama, [d]Human Health Sciences, Graduate School of Medicine, Kyoto University, Kyoto, Departments of [e]Gastroenterology and Hepatology, [f]Internal Medicine and [g]Clinical Laboratory, Kaizuka City Hospital, Kaizuka, [h]Department of Gastroenterology and Hepatology, Japan Labour Health and Welfare Organization, Kansai Rousai Hospital, Amagasaki, and [i]Department of Gastroenterology and Hepatology, Osaka University Graduate School of Medicine, Suita, Japan

Key Words

Real-time tissue elastography · Chronic hepatitis · Ultrasound elastography · Liver fibrosis

Abstract

It has been established that the long-term infection of chronic hepatitis C leads to the increased risk of hepatic fibrosis and hepatocellular carcinoma. Currently, histological diagnosis by invasive and painful liver biopsy is the gold standard for evaluating the hepatic fibrosis stage. Because of a side effect or patient inability to cope with the pain, it is difficult to assess the fibrosis stage frequently using liver biopsy. Recently, instead of liver biopsy, many articles have been published showing the usefulness of ultrasound elastography to evaluate the stage of hepatic fibrosis. We also reported the usefulness of real-time tissue elastography (RTE) for liver fibrosis staging in 2007. However, in our previous report, fibrosis classification was performed manually and the number of patients involved was also small. In the current study, the fibrosis staging is performed automatically using software by characterizing the elastography images. We have also increased the number of patients from 64 to 310. Thus, the aim of this study is to increase objectivity by using a newly developed automatic analysis method. We obtain the Liver Fibrosis Index (LFI), which is calculated from image features of RTE images, using multiple regression analysis performed on clinical data of 310 cases as the training data set. The correlation coefficient obtained between the LFI and the stage of hepatic fibrosis was $r = 0.68$, and significant differences exist between all stages of fibrosis ($p < 0.001$). Our new method seems promising since it has the ability to diagnose fibrosis even in the presence of inflammation.

Introduction

Approximately 700,000 people worldwide are estimated to die annually of hepatocellular carcinoma (HCC), which is the third highest cause of cancer death [1, 2]. HCC often develops in the presence of hepatic fibrosis from long-term infection of chronic hepatitis B and C. It has been reported that the risk of HCC increases as the stage of liver fibrosis progresses [3]. It has been shown that fibrosis treatment using interferon reduces hepatic

KARGER

Fax +41 61 306 12 34
E-Mail karger@karger.com
www.karger.com

0030–2414/13/0847–0003$38.00/0

Accessible online at:
www.karger.com/ocl

Masatoshi Kudo, MD, PhD
Division of Gastroenterology and Hepatology, Department of Internal Medicine
Kinki University Faculty of Medicine
377-2 Ohno-Higashi, Osakasayama, Osaka 589-8511 (Japan)
E-Mail m-kudo@med.kindai.ac.jp

Abbreviations used in this paper

MEAN	Mean of relative strain value within the ROI
SD	Standard deviation of relative strain value within the ROI
%AREA	Area of low strain (blue) within the ROI
COMP	Complexity of low strain (blue) area within the ROI = (perimeter)^2/area
SKEW	Skewness – asymmetry of the histogram
KURT	Kurtosis – peakedness of the histogram
ENT	Entropy – textural complexity
IDM	Inverse Difference Moment – textual local homogeneity
ASM	Angular Second Moment – textual homogeneity

fibrosis and also dramatically reduces the incidence of HCC [4]. Thus, it is important to evaluate the stage of hepatic fibrosis both for establishing treatment and also for monitoring its effectiveness.

Histological diagnosis using liver biopsy is very important for the evaluation of hepatic fibrosis [5–10]. However, because of its invasiveness, liver biopsy cannot be performed frequently. In addition, there is a limitation in the accuracy of liver biopsy due to sampling error [11–13]. Thus, the development of noninvasive tests that are reliable, cost-effective and easy to use is required for evaluating the stage of hepatic fibrosis. Previously, measurement of platelet counts [14] and liver fibrosis marker [15–18] were used as noninvasive tests to evaluate hepatic fibrosis, but generally the basic procedure for evaluating the stage of hepatic fibrosis is to combine the use of these tests with diagnostic imaging techniques, such as ultrasonography.

Ultrasound imaging is the most useful imaging diagnostic technique used for evaluating chronic hepatitis and/or cirrhosis. The image characteristics for evaluating hepatic fibrosis/cirrhosis are the nodular liver parenchyma, heterogeneous internal echo texture, decrease in the volume of right hepatic lobe and increase in the volume of caudate and left hepatic lobe, and the narrowing of the hepatic vein [19, 20]. However, staging of the liver fibrosis using these characteristics is less reliable since the appearance of images can be changed due to differences in ultrasonic power and/or the image settings of the equipment used. Ultrasound tissue characterization has been attempted in the literature for objective evaluation of tissue by analyzing the signals obtained from the ultrasound system, for example intensity of RF signals, extent of scattering [21, 22] and velocity of shear wave generated by a probe in the liver [23].

New methods are emerging to estimate the liver stiffness or the fibrosis, using ultrasound elastography or MRI [24]. There are many forms of elastography that are popular, namely transient elastography (Fibroscan®) [25–28], acoustic radiation forces impulse imaging (ARFI) and our own real-time tissue elastography (RTE) [29–32]. Fibroscan and ARFI measure the velocity of shear waves propagating in the tissue to measure liver stiffness, which is then correlated to fibrosis. However, in the case of Fibroscan, measured liver stiffness is correlated not only with the stage of hepatic fibrosis, but also with grade of inflammation. Therefore, the involvement of many dynamic factors independent of hepatic fibrosis affect the measurement value, such as inflammation or cholestasis. The stage of hepatic fibrosis, which is the goal of the imaging technique, should be defined as the parameter dependent only on the fibrosis of the liver, which is the true pathology to be indicated and should not include other dynamic factors.

Our RTE is different from Fibroscan and ARFI and it measures relative stiffness of the tissue in the region of interest (ROI) and displays the stiffness with color overlaid over the B-mode image in real time. Apart from liver imaging, it has many other clinical applications that have been reported in the literature, such as breast, thyroid, prostate and pancreas [33–36]. RTE image is constructed using tissue strains which are calculated from 2 consecutive frames. The phase difference of RF signals from 2 consecutive frames are calculated to obtain tissue strain and transferred to color codes. The colors in the ROI range from blue to red to show the relative hardness and softness of area inside the ROI [30, 31]. The harder areas are displayed in blue and the softer areas in red.

In our previous work using RTE for liver imaging, we established the usefulness of RTE for the evaluation of hepatic fibrosis of chronic hepatitis C patients. The reported liver elasticity scores, which were scored visually, showed significant correlation with hepatic fibrosis [37]. Our RTE, available as a native mode in an ultrasound system, can be used for evaluating patients even with ascites and severe hepatic atrophy.

Even though our previous paper showed the feasibility of using RTE, the main limitation was that the evaluation of the RTE images was performed visually. While evaluating visually, two radiologists used the increase in a blue area in the RTE image as a criteria for staging hepatic fibrosis. Blue areas of RTE images increased and became patchy as the stage of hepatic fibrosis increased. It was difficult for the radiologists to visually estimate hepatic fibrosis with RTE images since the scoring of fibrosis also depended on the individual examiner's image perspective. In addition, in our previous report, we did not perform any investigation about the relationship between the grade of inflammation and the RTE image. Thus, the aims of this study are: (1) to present a newly developed

image analysis software method to obtain Liver Fibrosis Index (LFI) automatically from image features of RTE images using multiple regression analysis [38–40], (2) to show the effectiveness of this software tool and (3) to establish the relationship between LFI, the stage of fibrosis and the grade of inflammation.

Patients and Methods

Patients

The protocol was created following the Declaration of Helsinki and approved by an independent ethics committee of 3 institutions. For this study, we chose 295 patients with chronic hepatitis C or cirrhosis. Fifty-five patients were excluded from the study (table 1). All these patients were anti-hepatitis C virus and hepatitis C virus RNA positive, and were diagnosed by liver biopsy between May 2005 and December 2009. The patient population included 130 males and 165 females aged between 26 and 76 years old (mean age 56 years; table 1). Fifteen healthy volunteers were also enrolled as a normal control group. We obtained written informed consent from all participants at the National Hospital Organization Minamiwakayama Medical Center, Kaizuka City Hospital and Kinki University Hospital.

Liver Histology

Liver biopsy was performed twice using 18G automatic cutting biopsy needles (Adjustable Temno Biopsy System; Cardinal Health, Waukegan, Ill., USA) under local anesthesia for all study patients. Regardless of benign or malignant tumor, patients who had tumor located in the imaging plane from the right intercostal were excluded from the study. The specimen lengths were 20 mm (range 10–25 mm) and the sections were stained with hematoxylin and eosin and Masson trichrome staining. These sections were examined by 3 pathologists to stage the fibrosis and also to grade the activities. All 3 pathologists were blinded to any clinical data including the results of RTE. Hepatic fibrosis were staged from F0 to F4 according to the following scale: F0 – no fibrosis, F1 – portal fibrosis without septa, F2 – portal fibrosis with septa, F3 – numerous septa without cirrhosis and F4 – cirrhosis. Inflammatory activities were graded from A0 to A3 with the following scale: A0 – no activity, A1 – mild activity, A2 – moderate activity and A3 – severe activity.

The fifteen healthy volunteers were all male, aged between 22 and 52 years (average 31.5), BMI between 17.9 and 24.7 (average 21.0) and their blood tests, such as aspartate aminotransaminase, alanine transaminase, gamma-GTP, total cholesterol and triglyceride, were all within normal limits. All volunteers had no sign of fatty liver in ultrasonography findings, thus no liver biopsy was performed and they were staged F0.

Real-Time Tissue Elastography

HI VISION 900 (Hitachi Medical Corp., Tokyo, Japan) was used for ultrasonography and the probes used were EUP-L52 linear probes (7–3 MHz). We used linear array probes for this study over convex array probes because linear probes have many advantages when internal compression and relaxation induced by the cardiac motion is utilized for obtaining RTE images of the liver. We utilized internal compression and relaxation induced by the cardiac motion instead of manual compression because this is more consistent and reliable. Even though the field of view of a linear array probe is small, the direction of displacement induced by cardiac movement can be set to the surface of the probe, thus making it suitable for RTE analysis. Also, at smaller depth the field of view of a linear probe is much larger than that of convex probes, thus making it more suitable for an RTE image.

After obtaining B-mode images, the ultrasound mode was switched to RTE and scanned from the right intercostal space to observe the right hepatic lobe. RTE images were obtained by holding the probe still at the position where displacement by the cardiac motion in B-mode was in the axial direction. The optimum intercostal space was the position where liver parenchyma was imaged in the deepest area. When the liver was not contracted, RTE images were easily obtained by scanning through the intercostal space of anterior to middle axillary lines. Because the RTE image is formed from the strain values computed from the axial displacement, the position where liver parenchyma moves in a lateral direction due to cardiac motion was not suitable for this study.

The ROI for RTE was set inside liver parenchyma. Regions with large vessels or regions having shadows from ribs were avoided to reduce the artifacts arising from the anechoic region. The tops of the ROI were positioned at a depth of more than 1 cm from the surface of the liver to avoid multiple reflections arising from the surface of the liver.

RTE was performed using a freehand technique, with the linear probe placed at the appropriate position with the patient holding their breath. As mentioned in the previous paragraph, no manual compression/relaxation was applied. The compression/

Table 1. Background of patients and excluded cases

Patients (n = 295)	
Male/female	130/165
Age, years	56 ± 18
Range	26 – 76
ALT, IU/l	59.4 ± 41.1
Total bilirubin, mg/dl	0.9 ± 0.5
Albumin, g/dl	4.0 ± 1.1
Choline esterase, IU/l	270.4 ± 78.4
Total cholesterol, mg/dl	187.4 ± 33.4
Prothrombin time, %	94.2 ± 12.9
Platelet count ($\times 10^4/\mu l$)	16.2 ± 7.7
Fibrosis stage, F0/F1/F2/F3/F4	84/97/65/48
Histological activity, A0/A1/A2/A3	29/90/146/30
Excluded cases (n = 55)	
Poor penetration (n = 20)	
Fatty layer ≥5 mm and muscular layer ≥10 mm	9
Fatty layer ≥5 mm and muscular layer <10 mm	3
Fatty layer <5 mm and muscular layer ≥10 mm	5
Fatty layer <5 mm and muscular layer <10 mm	3
Unstable technique (n = 35)	
Slipping section by body movement	10
Slipping horizontally by cardiac movement	13
Poor cardiac movement	3
Artifact by multiple reflection	9

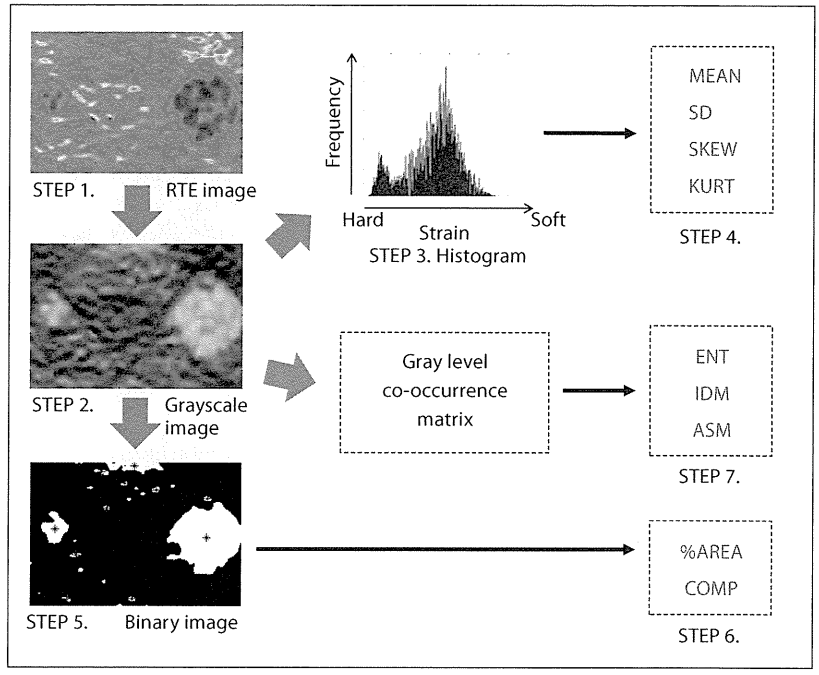

Fig. 1. Flow of calculations.

relaxation of the liver induced by the cardiac motion is easily detected to compute strain images. The ultrasound system parameters such as depth, ROI and gain were set for optimum RTE image quality. RTE images obtained by the lateral movements of the heart were avoided. One to two RTE images are displayed in 1 heartbeat, and the best RTE image was selected for final analysis. In total 3–5 RTE images obtained from different heart cycles without lateral motion were selected. The average of these 3–5 images for each patient was then used in regression analysis.

We extracted the following 9 image features to quantify the patchy pattern of the RTE images. More details about these features can also be found in the literature [41].

All 9 parameters have been found in the literature to be very useful for characterizing the imaging pattern in many different applications, e.g. satellite imaging, geothermal imaging and machine visions [42]. For liver fibrosis staging using RTE images, we employ these features for characterizing the image and correlating them with fibrosis staging. Analysis of RTE image features were performed with the prototype analysis software shown in figure 1. This software converts the selected analysis area of the RTE image (STEP 1) into a 256-step grayscale image (STEP 2), plots the strain histogram (STEP 3), and calculates the mean of relative strain (MEAN), standard deviation of relative strain (SD), skewness of strain histogram (SKEW) and kurtosis of strain histogram (KURT; STEP 4). Moreover, it binarizes the RTE image into black and white regions: white as low strain (blue) regions and black as all other regions (STEP 5). To characterize the low strain (blue) regions of the binary image, it calculates the ratio of low strain regions within the selected analysis area (%AREA), and the complexity of the low strain region (COMP; STEP 6). Furthermore, it also calculates entropy (ENT), inverse difference moment (IDM), and angular second moment (ASM) to evaluate the texture of the RTE image (STEP 7). Multiple regression analysis was then performed to improve the diagnostic accuracy using all these 9 image features instead of diagnosing with individual image features.

The LFI was estimated using these 9 image features as independent variables and the hepatic fibrosis stage as a dependent variable, as shown in the following multiple regression equation:

$$\begin{aligned}\text{LFI} = {} & -0.009 \times \text{MEAN} - 0.005 \times \text{SD} + 0.023 \times \%\text{AREA} \\ & + 0.025 \times \text{COMP} + 0.775 \times \text{SKEW} - 0.281 \times \text{KURT} \\ & + 2.083 \times \text{ENT} + 3.042 \times \text{IDM} + 39.979 \times \text{ASM} - 5.542.\end{aligned}$$

Multiple regression analysis was also performed to estimate the Liver Activity Index (LAI) using 9 image features as independent variables and grade of inflammatory activity as a dependent variable. LFI and LAI were calculated for all patients and compared with the stage of hepatic fibrosis and grade of inflammatory activity. Then, to eliminate the inflammatory activity from hepatic fibrosis, LAI and grade of inflammatory activity were compared for each stage of hepatic fibrosis. Receiver operating characteristic (ROC) analysis was performed for LFI to obtain a cutoff value for the identification of F0–1/F2–4 and F0–3/F4, and also to calculate sensitivity, specificity, accuracy and area under ROC (AUROC).

Statistical Analysis

All of the statistical analysis, such as multiple regression analysis and ROC analysis were carried out using the JMP statistical discovery software, version 8.0 (SAS Institute Inc., Cary, N.C., USA) for windows.

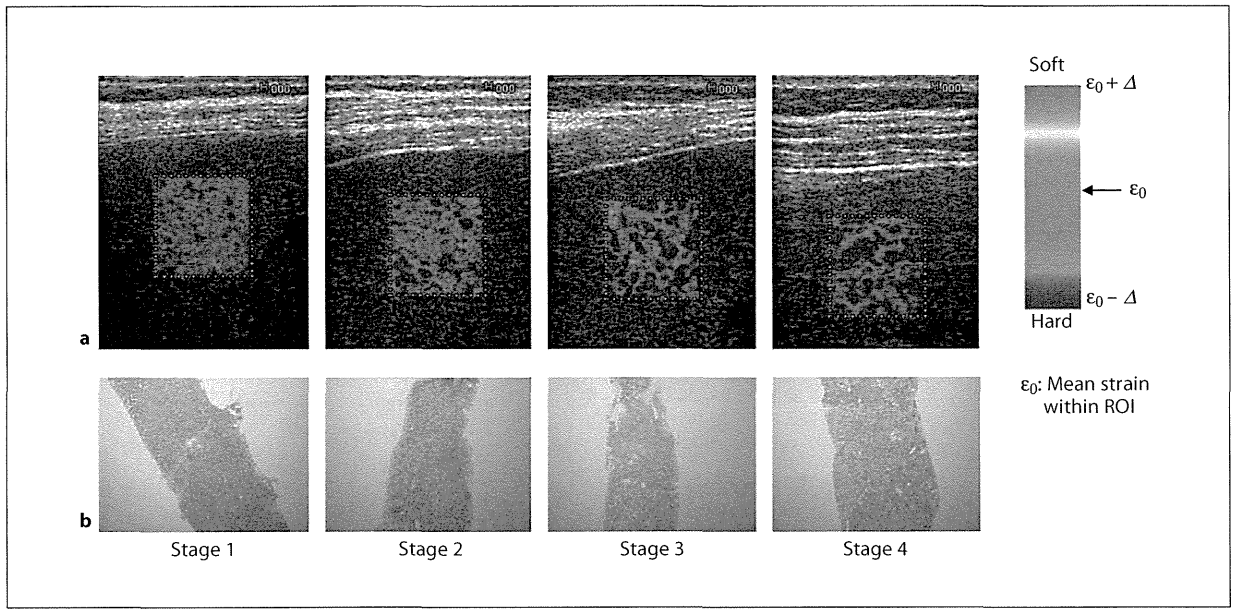

Fig. 2. RTE images (**a**) and pathological images, Masson trichrome stain, ×100 (**b**).

Results

Patients

We performed liver elastography in 365 patients (including 15 healthy volunteers) between April 2005 and November 2009. We excluded 55 patients from our study because more than 3 stable RTE images could not be acquired for these patients. Most of the reasons of exclusion were related to RTE skill of the clinicians, which improved significantly with more experience. Table 1 shows the characteristics of the 295 patients (excluding 15 healthy volunteers out of 310 patients). The indicated stages of hepatic fibrosis in the study patients were: F0 in 1 subject, F1 in 84 subjects, F2 in 97 subjects, F3 in 65 subjects and F4 in 48 subjects. The stage of hepatic fibrosis in all healthy volunteers was F0. Typical RTE images and pathological images for each fibrosis stage are shown in figure 2.

Correlation between Features and Stage

In the present study, as described previously, we extracted 9 image features. Correlation coefficients between 9 image features, such as MEAN, SD, %AREA, COMP, SKEW, KURT, ENT, IDM and ASM and stage of hepatic fibrosis were −0.63, 0.53, 0.65, 0.58, 0.59, 0.02, −0.22, 0.34 and 0.21, respectively. Thus, 5 of 9 image features, i.e. MEAN, SD, %AREA, COMP and SKEW, highly correlated with the stage of hepatic fibrosis (fig. 3).

Accuracy of Staging Fibrosis by LFI

Figure 4 shows the relationship between hepatic fibrosis stages and LFI calculated from 9 image features using multiple regression analysis. LFI highly correlates with the fibrosis stages ($r = 0.68$ with $p < 0.001$), and significant differences exist between all different stages. Figure 5 shows the ROC analysis. When the cutoff value of LFI was set to 1.92, the AUROC of LFI for F0–1 versus F2–4 was 0.82, and sensitivity, specificity and accuracy were 78.6, 78.0 and 78.4%, respectively. For F0–3 versus F4, when the cutoff value was 2.56, the AUROC was 0.87, and sensitivity, specificity and accuracy were 79.2, 80.5 and 80.3%, respectively (fig. 5). In this study, LFI clearly differentiates either F0–1 and F2–4 or F0–3 and F4.

Effect of Inflammation

Figure 6 shows the comparison between grades and the 9 image features for evaluating the effect of inflammation on RTE image. None of the 9 image features have a correlation with grades, and LAI, which was calculated by multiple regression analysis similar to LFI, also did not correlate with grades ($r = 0.30$; fig. 6j).

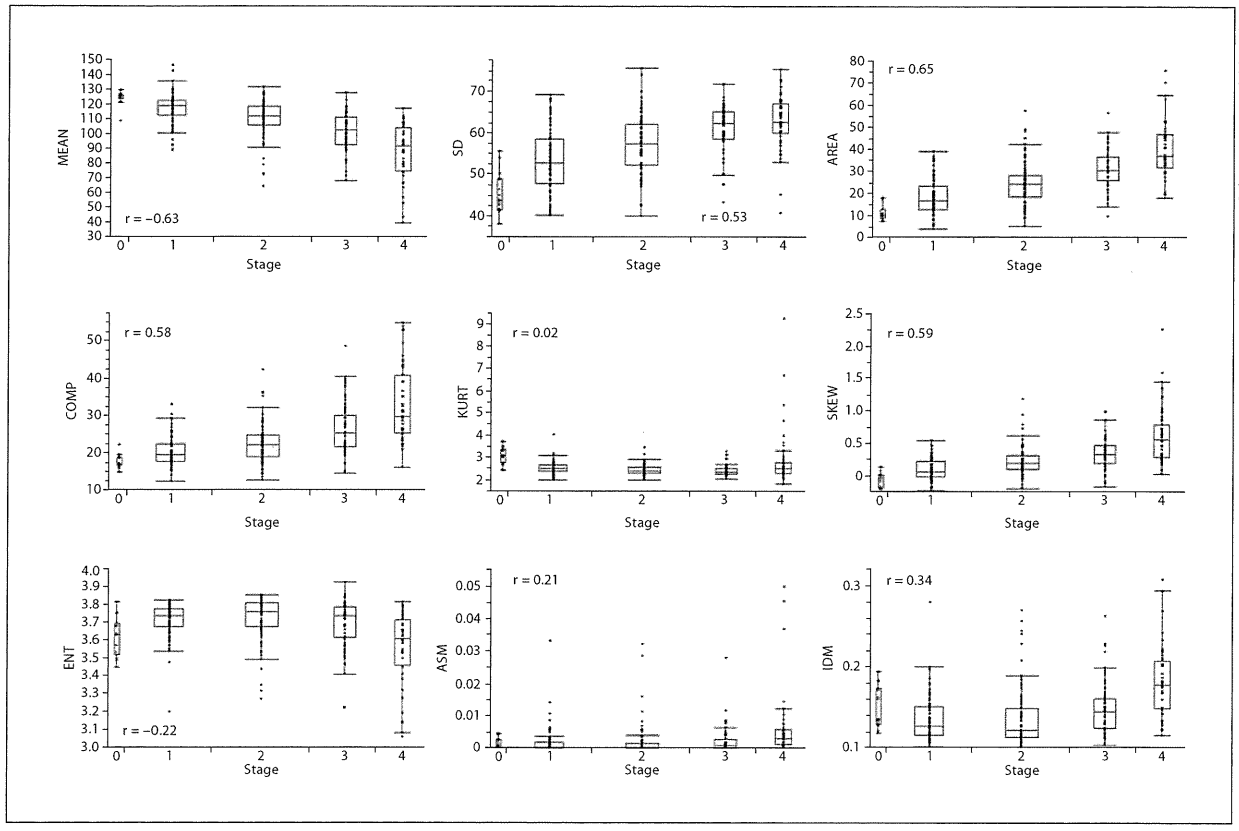

Fig. 3. Comparisons of stage of hepatic fibrosis and image features.

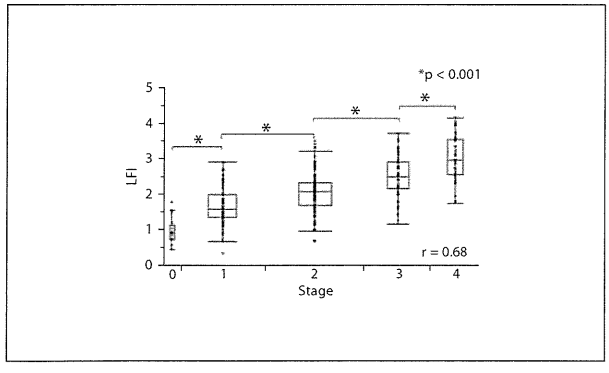

Fig. 4. Comparison of stage of hepatic fibrosis and LFI.

Discussion

Results of Estimation

To improve the accuracy of estimation of hepatic fibrosis and to make it automatic, we performed multiple regression analysis using 9 image features and obtained the estimated LFI. This index highly correlated with the stage of hepatic fibrosis ($r = 0.68$, $p < 0.001$) and significant differences were also observed between each stage. Furthermore, ROC analysis indicated that LFI has a high ability to differentiate each stage.

All 9 image features we used are independent and do not include confounding factors. Out of the 9 image features we analyzed, 5 (%AREA, MEAN, SD, COMP and SKEW) had a high correlation with the stages of hepatic fibrosis. This strong correlation, we believe, is mainly due to following reasons:

- AREA: hard area increases as a hepatic fibrosis progresses.

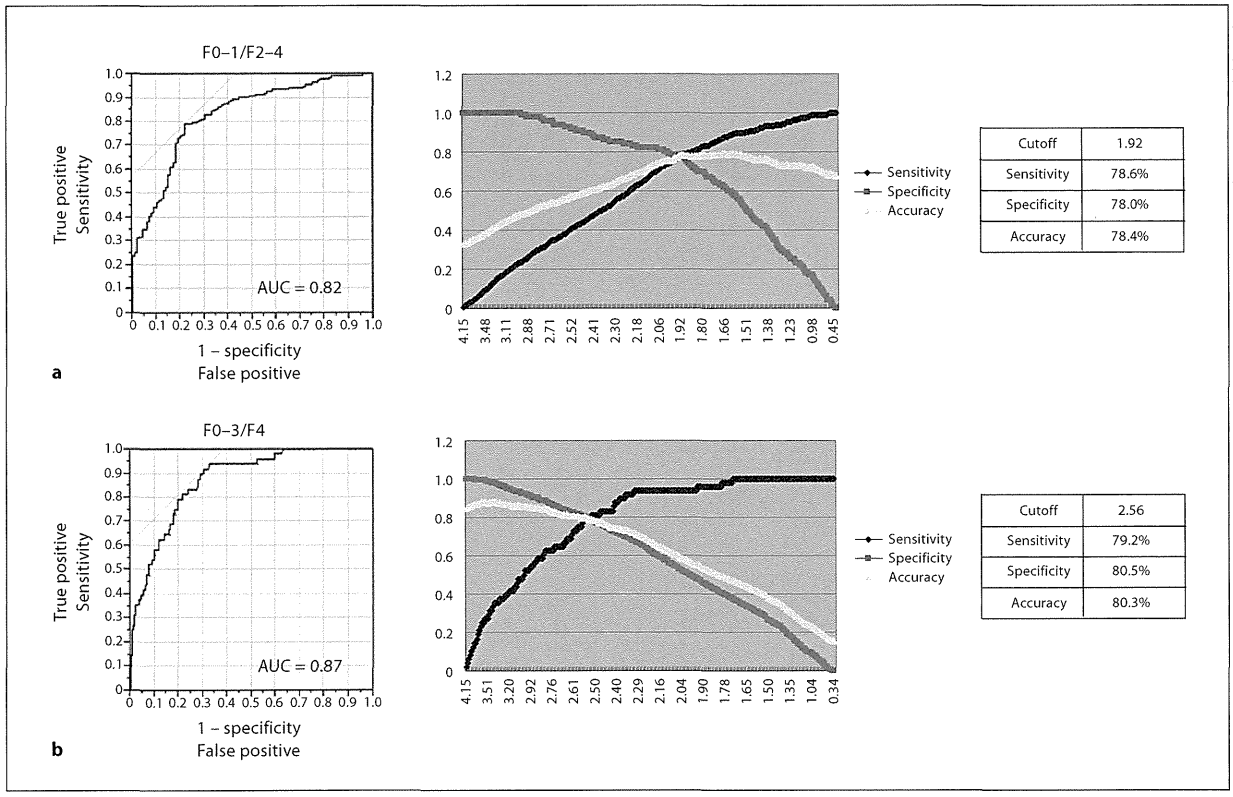

Fig. 5. ROC analysis differentiating F2–4 from F0–1 (**a**) and F4 from F0–3 (**b**).

- MEAN: liver parenchyma becomes stiffer as hepatic fibrosis progresses.
- SD: stiffness of liver parenchyma becomes heterogeneous as hepatic fibrosis progresses.
- COMP: figure of hard area becomes more complex as hepatic fibrosis progresses.
- SKEW: histogram skew towards the lower value of strain (harder) as hepatic fibrosis progresses.

Histopathological tissue evaluation using liver biopsy has been the gold standard for evaluation of hepatic fibrosis. However, this procedure is invasive, painful and could cause complications, such as hemorrhage, due to which many patients hesitate over the procedure. In addition, if the platelet count is low, partial thromboplastin time is greater than 3 s, the liver presents with a tumor and there is presence of ascites, then liver biopsy is also difficult to perform. This liver biopsy is also an economic burden due to the hospitalization required after the procedure. Currently, in such patients where a liver biopsy cannot be performed it is substituted with blood tests, which have significantly lower accuracy. Thus, our LFI based on RTE images, which is painless, cost-effective and can be performed in the presence of any of the above conditions can be a good addition to the clinicians tools for the noninvasive evaluation of liver fibrosis.

Effect of Inflammation

We did not find any correlation between any of the 9 features we used and inflammation grades. The RTE image, we believe, thus reflects the hepatic fibrosis and does not reflect the inflammatory factors such as intracellular pressure and change in blood flow due to inflammation. In addition, the spatial resolution of RTE images is 0.5–2 mm [43], which can completely capture the regenerating nodules in liver cirrhosis, which are 3–10 mm in size [44]. Thus, we can conclude that the LFI we have developed is not influenced by inflammation and it depends mainly upon liver fibrosis. Compared to RTE, other shear wave elastogra-

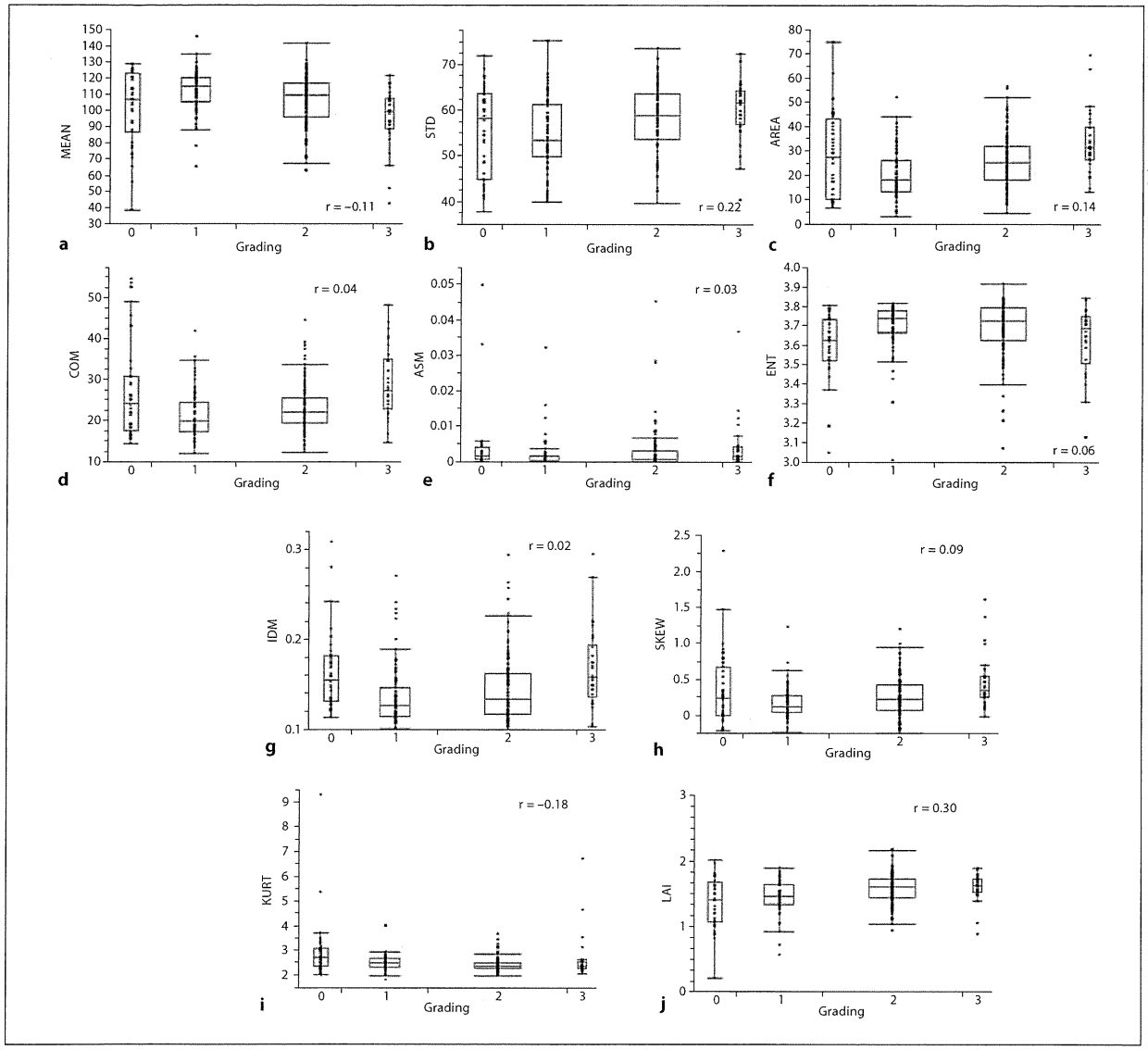

Fig. 6. a–j Comparison of grade and image features.

phy-based techniques, such as Fibroscan and ARFI, have been reported showing strong correlation with inflammation [45–47]. This correlation could be mainly because shear wave elastography adopts the principle of measuring the velocity of shear wave. Inflammatory factors such as intracellular pressure and condition of blood flow may change the velocity of shear waves, thus resulting in bias in the estimate.

Acquisition of RTE

We utilized compression/relaxation induced by the cardiac motion to obtain our RTE images for liver index computation. This helped to simplify RTE image acquisition and made it easier for clinicians to acquire RTE images. However, for some patients with weak pulsation and/or who are obese, it was difficult to perform liver elastography accurately. Training of clinicians was needed to avoid artifacts related to obesity, to set the ROI not

to include vessels and to adjust the position of the probe to image the liver where compression/relaxation was homogeneous and axial to the probe. RTE data were collected in 3 hospitals and 2 experts performed liver elastography. Image features were extracted from multiple RTE images and the average value from the acquired RTE images were used for our analysis.

Patient Selection Bias

In our study we did not include patients who had difficulty holding their breath or for whom it was difficult to image the liver through the intercostal spaces due to overlying bowel gases. Moreover, we excluded 55 cases with difficulty in analysis, the reasons for which are shown in table 1. The acquisition rate was 84.9% (310/365), which is still quite impressive in spite of these exclusions. Most of the exclusions happened at the beginning of the study. As the clinician gained experience, the failure rate reduced significantly and the success rate increased up to 98.0% (98/100). This implies that with some education and training the acquisition failure rate can be decreased significantly.

Limitations

We compared the results of LFI derived from RTE images with histopathological results of liver biopsy. However, liver biopsy results themselves have bias due to sampling error and due to the histopathological image being classified not by continuous quantity but staged by the progression of hepatic fibrosis. Moreover, there are large differences in the progression of hepatic fibrosis between 4 stages of liver fibrosis [40], thus the accuracy of liver biopsy is limited. Since liver biopsy results are used as a training set for our LFI computation, we speculate that there is also some bias in our estimate of liver fibrosis. A new index is needed as training data to derive a multiple regression equation to reduce the variation in results.

As a future subject for increasing the accuracy of the LFI, fibrosis staging by two or more pathologists is due to be judged using the block specimen by a surgical resection. Thereby, since the variation in a pathology result can be decreased, we think that better equation estimates of LFI can be derived.

Prospects of RTE

Our results of liver fibrosis staging are very impressive. It is automatic, consistent and agrees very well with current liver biopsy results. Thus, in the near future, we expect that the RTE could be used as a first-choice imaging tool for fibrosis screening. If considered suspicious, then liver biopsy can be performed for further confirmation. In addition, RTE imaging could be the only choice available along with blood tests for patients in whom liver biopsy cannot be performed. RTE can also be used for monitoring the progress or resolution of fibrosis in patients treated with interferon. It can also be used to monitor the progress in fibrosis in patients where interferon treatment was not done. RTE imaging is easy to use, cost-effective and, moreover, painless. It is readily available with the ultrasound machine as an additional mode making the technique easily available and easy to use when liver screening is being done to monitor cirrhosis and rule out HCC. It can also be used in patients with hepatitis other than viral, such as nonalcoholic steatohepatitis, etc.

Conclusion

LFI computed from RTE images highly correlates with stages of hepatic fibrosis and accurately reflects the underlying hepatic fibrosis, even with the presence of inflammation. Thus, it can be used for screening, monitoring and at times diagnosis of hepatic fibrosis. We believe our results and our techniques are superior to other techniques such as transient elastography. In the near future we plan to conduct more extensive clinical studies both for substantiating our results as well as to prove the clinical utility of RTE imaging for liver fibrosis staging.

Acknowledgments

We would like to thank Akiko Tonomura, Tsuyoshi Mitake, Mitsuru Motoki, Tomoko Furuta, MD, Chie Tatsumi, MD, Shigeo Wada, MD and Masahide Oshita, MD, for valuable contributions to this study.

Disclosure Statement

The authors declare that no conflicts of interest exist.

References

1 WHO International Agency for Research on Cancer: World Cancer Report 2008. Section 1 – global cancer control, chapter 1.3: worldwide cancer burden. http://www.iarc.fr/en/publications/pdfs-online/wcr/2008/index.php.

2 WHO International Agency for Research on Cancer: World Cancer Report 2008. Section 2 – etiology of cancer, chapter 2.5: chronic Infections.

3 Yoshida H, Shiratori Y, Moriyama M, et al: Interferon therapy reduces the risk for hepatocellular carcinoma: national surveillance program of cirrhotic and noncirrhotic patients with chronic hepatitis C in Japan. Ann Intern Med 1999;131:174–181.
4 Shiratori Y, Imazeki F, Moriyama M, et al: Histologic improvement of fibrosis in patients with hepatitis C who have sustained response to interferon therapy. Ann Intern Med 2000;132:517–524.
5 Desmet VJ, Gerber M, Hoofnagle JH, et al: Classification of chronic hepatitis: diagnosis, grading and staging. Hepatology 1994; 19:1513–1520.
6 Ichida F, Tsuji T, Omata M, et al: Classification report: new inuyama classification for histological assessment of chronic hepatitis. Internat Hepatol Comm 1996;6:112–119.
7 Ishak K, Baptista A, Bianchi L, et al: Histological grading and staging of chronic hepatitis. J Hepatol 1995;22:696.
8 Bataller R, Brenner DA: Liver fibrosis. J Clin Invest 2005;115:209–218.
9 Pinzani M, Rombouts K, Colagrande S: Fibrosis in chronic liver diseases: diagnosis and management. J Hepatol 2005;42:S22–S26.
10 Dienstag JL: The role of liver biopsy in chronic hepatitis C. Hepatology 2002;36: S152–S160.
11 Gebo KA, Herlong HF, Torbenson MS, et al: Role of liver biopsy in management of chronic hepatitis C: a systemic review. Hepatology 2002;36:161–172.
12 Regev A, Berho M, Jeffers LJ, Milikowski C, et al: Sampling error and intraobserver variation in liver biopsy in patients with chronic HCV infection. Am J Gastroenterol 2002;97: 2614–2618.
13 Bedossa P, Dargère D, Paradis V: Sampling variability of liver fibrosis in chronic hepatitis C. Hepatology 2003;38:1449–1457.
14 Omata M: A strategy of the treatment for the viral hepatitis (in Japanese). J Jpn Soc Int Med 2004;93:269–276.
15 Manning DS, Afdhai NH: Diagnosis and quantitation of fibrosis. Gastroenterology, 2008;134:1670–1681.
16 Wai CT, Greenson JK, Fontana RJ, et al: A simple noninvasive index can predict both significant fibrosis and cirrhosis in patients with chronic hepatitis C. Hepatology 2003; 38:518–526.
17 Imbert-Bismut F, Ratziu, Pieroni L, Charlotte F, et al: Biochemical markers of liver fibrosis in patients with hepatitis C virus infection: a prospective study. Lancet 2001;357: 1069–1075.
18 Forns X, Ampurdanes S, Llovet JM, et al: Indentification of chronic hepatitis C patients without hepatic fibrosis by a simple predictive model. Hepatology 2001;36:986–992.
19 Freeman MP, Vick CW, Taylor KJ, et al: Regenerating nodules in cirrhosis: sonographic appearance with anatomic correlation. AJR Am J Roentgenol 1986;146:533–536.
20 Ishikawa H, Ono M, Goto M, et al: Ultrasonographic findings in patients with liver cirrhosis; relationships between parenchymal, superficial echo patterns, and histological findings (in Japanese). Jpn J Med Ultrason 1990;17:522–529.
21 Fujimoto K, Yamamoto Y, Waki H, et al: Tissue characterization using integrated backscatter in viral chronic liver disease. J Ultrasound Med 1999;18(suppl):472.
22 Kumada T, Toyoda H, Ogawa S, et al: Quantification of fibrosis in hepatitis C using statistics analysis tool of ultrasonics (2nd report). Jpn J Med Ultrasonics 2007;34:S641.
23 Ziol M, Handra-Luca A, Kettaneh A, et al: Noninvasive assessment of liver fibrosis by measurement of stiffness in patients with chronic hepatitis C. Hepatology 2005;41:48–54.
24 Joo I, Choi BI: New Paradigm for management of hepatocellular carcinoma by imaging. Liver Cancer 2012;1:94–109.
25 Sandrin L, Fourquet B, Hasquenoph JM, et al: Transient elastography: a new noninvasive method for assessment of hepatic fibrosis. Ultrasound Med Biol 2003;29:1705–1713.
26 Foucher J, Chanteloup E, Vergniol J, et al: Diagnosis of cirrhosis by transient elastography (FibroScan): a prospective study. Gut 2006;55:403–408.
27 Fraquelli M, Rigamonti C, Casazza G, et al: Reproducibility of transient elastography in the evaluation of liver fibrosis in patients with chronic liver disease. Gut 2007;56:968–973.
28 Kim DY, Kim SU, Park JY, Ahn SH, Song KJ, Han KH: FibroScan based risk estimation of HBV-related HCC occurrence: development and validation of a predictive model. Liver Cancer 2012;1:123.
29 Friedrich-Rust M, Wunder K, Kriener S, et al: Liver fibrosis in viral hepatitis: noninvasive assessment with acoustic radiation force impulse imaging versus transient elastography. Radiology 2009;252:595–604.
30 Shiina T, Nitta N, Ueno E, et al: Real time tissue elasticity imaging using the combined autocorrelation method. J Med Ultrasonics 1999;26:57–66.
31 Shiina T, Nitta N, Ueno E, et al: Real time tissue elasticity imaging using the combined autocorrelation method. J Med Ultrasonics 2002;29:119–128.
32 Joo I, Choi BI: New paradigm for management of hepatocellular carcinoma by imaging. Liver Cancer 2012;1:94–109.
33 Itoh A, Ueno E, Tohno E, et al: Breast disease: clinical application of US elastography for diagnosis. Radiology 2006;239:341–350.
34 Fukunari N: More accurate and sensitive diagnosis for thyroid tumors with elastography – detection and differential diagnosis of thyroid cancers. MEDIX Suppl. 2007. http://www.hitachi-medical.co.jp/tech/medix/pdf/supple/sup_05.pdf.
35 Tsutsumi M, Miyagawa T, Matsumura T, et al: Real-time balloon inflation elastography for prostate cancer detection and initial evaluation of clinic pathologic analysis, AJR Am J Roentgenol 2010;194:W471–W476.
36 Hirooka Y, Itoh A, Kawashima H, et al: Diagnosis of pancreatic disorders using contrast-enhanced endoscopic ultrasonography and endoscopic elastography. Clin Gastroenterol Hepatol 2009;7:S63–S67.
37 Fujimoto K, Wada S, Oshita M, et al: Noninvasive evaluation of hepatic fibrosis in patients with chronic hepatitis C using elastography. MEDIX Suppl. 2007. http://www.hitachi-medical.co.jp/tech/medix/pdf/supple/sup_07.pdf.
38 Tatsumi C, Kudo M, Ueshima K, et al: Noninvasive evaluation of hepatic fibrosis using serum fibrotic markers, transient elastography (FibroScan), and real-time tissue elastography. Intervirology 2008;1:S27–S33.
39 Tatsumi C, Kudo M, Ueshima K, et al: Noninvasive evaluation of hepatic fibrosis for type C chronic hepatitis. Intervirology 2010; 53:76–81.
40 Fujimoto K, Kato M, Tonomura A, et al: Non-invasive evaluation method of the liver fibrosis using real-time tissue elastography – usefulness of judgment liver fibrosis stage by Liver Fibrosis Index (LF Index) (in Japanese). Kanzo 2010;51:539–541.
41 Haralick RM, Shanmugan K, Dinstein I: Textural features for image classification. IEEE Trans Syst Man Cybern 1973;3:610–621.
42 Mittal D, Kumara V, et al: Neural network based focal liver lesion diagnosis using ultrasound images. Comp Med Imaging Graphics 2011;35:315–323.
43 Matsumura T, Shiina T, Oosaka T, et al: Development of real-time tissue elastography (in Japanese). MEDIX 2004;41:30–35.
44 Hoon L, Kim Y, Lee J: Regenerative nodules in liver cirrhosis: findings at CT during arterial portography and CT hepatic arteriography with histopathologic correlation. Radiology 1999;210:451–458.
45 Arena U, Vizzutti F, Abraldes JG, et al: Reliability of transient elastography for the diagnosis of advanced fibrosis in chronic hepatitis C. Gut 2008;57:1288–1293.
46 Vispo E, Barreiro P, Del Valle J, et al: Overestimation of liver fibrosis staging using transient elastography in patients with chronic hepatitis C and significant liver inflammation. Antivir Ther 2009;14:187–193.
47 Rifai K, Cornberg J, Mederacke I, et al: Clinical feasibility of liver elastography by acoustic radiation force impulse imaging (ARFI). Dig Liver Dis 2011;43:491–497.

J Gastroenterol (2012) 47:444–451
DOI 10.1007/s00535-011-0505-8

ORIGINAL ARTICLE—LIVER, PANCREAS, AND BILIARY TRACT

Decrease in alpha-fetoprotein levels predicts reduced incidence of hepatocellular carcinoma in patients with hepatitis C virus infection receiving interferon therapy: a single center study

Yukio Osaki · Yoshihide Ueda · Hiroyuki Marusawa · Jun Nakajima · Toru Kimura · Ryuichi Kita · Hiroki Nishikawa · Sumio Saito · Shinichiro Henmi · Azusa Sakamoto · Yuji Eso · Tsutomu Chiba

Received: 28 July 2011 / Accepted: 24 October 2011 / Published online: 23 November 2011

Abstract
Background Increasing evidence suggests the efficacy of interferon therapy for hepatitis C in reducing the risk of hepatocellular carcinoma (HCC). The aim of this study was to identify predictive markers for the risk of HCC incidence in chronic hepatitis C patients receiving interferon therapy.
Methods A total of 382 patients were treated with standard interferon or pegylated interferon in combination with ribavirin for chronic hepatitis C in a single center and evaluated for variables predictive of HCC incidence.
Results Incidence rates of HCC after interferon therapy were 6.6% at 5 years and 13.4% at 8 years. Non-sustained virological response (non-SVR) to antiviral therapy was an independent predictor for incidence of HCC in the total study population. Among 197 non-SVR patients, independent predictive factors were an average alpha-fetoprotein (AFP) integration value $\geq$10 ng/mL and male gender. Even in patients whose AFP levels before interferon therapy were $\geq$10 ng/mL, reduction of average AFP integration value to <10 ng/mL by treatment was strongly associated with a reduced incidence of HCC. This was significant compared to patients with average AFP integration values of $\geq$10 ng/mL ($P = 0.009$).
Conclusions Achieving sustained virological response (SVR) by interferon therapy reduces the incidence of HCC in hepatitis C patients treated with interferon. Among non-SVR patients, a decrease in the AFP integration value by interferon therapy closely correlates with reduced risk of HCC incidence after treatment.

Keywords Alpha-fetoprotein · Hepatocellular carcinoma · Hepatitis C · Interferon

Y. Osaki · J. Nakajima · T. Kimura · R. Kita · H. Nishikawa · S. Saito · S. Henmi · A. Sakamoto · Y. Eso
Department of Gastroenterology and Hepatology, Osaka Red Cross Hospital, 5-53 Fudegasaki-cho, Tennoji-ku, Osaka 543-8555, Japan

Y. Ueda (✉) · H. Marusawa · Y. Eso · T. Chiba
Department of Gastroenterology and Hepatology, Graduate School of Medicine, Kyoto University, 54 Kawahara-cho, Shogoin, Sakyo-ku, Kyoto 606-8507, Japan
e-mail: yueda@kuhp.kyoto-u.ac.jp

Introduction

Hepatitis C virus (HCV) infection is a predominant cause of liver cirrhosis and hepatocellular carcinoma (HCC) in many countries, including Japan, the United States, and countries of Western Europe [1–5]. The annual incidence of HCC in patients with HCV-related cirrhosis ranged from 1 to 8% [6–9]. Even in the absence of liver cirrhosis, patients with chronic hepatitis caused by HCV infection are at a high risk of developing HCC. Indeed, a large-scale Japanese cohort study showed that the annual incidence of HCC is 0.5% among patients with stage F0 or F1 fibrosis and 2.0, 5.3, and 7.9% among those with F2, F3, and F4 fibrosis, respectively [9]. Periodic surveillance is recommended to detect HCC as early as possible in patients with HCV-related chronic liver disease; however, this may not be cost-effective. For patients with chronic hepatitis C, more effective detection and prevention of HCC is being sought by two important routes: (1) the attempt to discover noninvasive predictive markers and (2) development of treatment strategies to reduce the risk of HCC. There have been several attempts to discover non-invasive markers capable of predicting the risk of HCC incidence in patients with chronic hepatitis C [6, 10]. For example, a cohort

derived from the Hepatitis C Antiviral Long-term Treatment Against Cirrhosis (HALT-C) Trial identified older age, African American race, lower platelet count, higher alkaline phosphatase, and esophageal varices as risk factors for HCC [11].

There have also been a number of studies to evaluate the effect of anti-viral treatment of chronic hepatitis C on the incidence of HCC [12–19]. The results were summarized in a meta-analysis, which concluded that the effect of interferon on risk of HCC is mainly apparent in patients achieving a sustained virological response (SVR) to interferon therapy [13]. In addition, a number of studies have suggested the incidence of HCC is reduced in treated patients compared to historical controls [12, 15, 16, 19]. However, the recent HALT-C randomized control trial revealed that long-term pegylated interferon therapy does not reduce the incidence of HCC among patients with advanced hepatitis C who do not achieve SVRs. Reduction in the risk of HCC by maintenance therapy was shown only in patients with cirrhosis [14, 17]. These controversial results suggest that interferon therapy reduces the risk of HCC only in a group of patients with HCV-related chronic liver disease. Thus, it is important to evaluate the risk of HCC development in hepatitis C patients receiving interferon therapy and it will be clinically useful to discover markers distinguishing high- and low-risk groups.

Serum alpha-fetoprotein (AFP) has been widely used as a diagnostic marker of HCC [20–22]. However, elevation of serum AFP levels is often found in non-neoplastic liver diseases without evidence of HCC, including acute liver injury and chronic viral hepatitis [23–27], especially among patients with advanced chronic hepatitis C [28]. An increase of AFP after liver damage is interpreted as a sign of dedifferentiated hepatic regeneration [27]. There have been some reports that AFP is a significant predictor of HCC in patients with chronic hepatitis C [4, 5, 29]. In addition, it has recently been shown that AFP levels decrease in response to interferon administration in patients with chronic hepatitis C [30, 31], and that long-term interferon therapy for aged patients with chronic HCV infection is effective in decreasing serum AFP levels and preventing hepatocarcinogenesis [32, 33]. However, little is known about the relationship between changes in serum AFP level over time during interferon therapy and the development of HCC.

The aim of this large single center study was to identify predictive markers for the risk of HCC development in patients receiving interferon therapy for chronic hepatitis C. For this purpose, patients treated with standard or pegylated interferon, in combination with ribavirin, for chronic hepatitis C were enrolled and subjected to scheduled periodic surveillance for HCC and a number of potential predictive markers, including AFP and alanine aminotransferase (ALT) integration values, at a single center.

Materials and methods

Patients

Between January 2002 and April 2010, 528 patients with chronic hepatitis C received combination therapy with standard interferon and ribavirin ($n = 84$) or pegylated interferon and ribavirin ($n = 444$) at Osaka Red Cross Hospital. Eligibility criteria for treatment were positivity for serum HCV RNA and histological evidence of chronic hepatitis C ($n = 427/444$; 80.9%), or positivity for serum HCV RNA, liver enzyme levels greater than the normal upper limit, and an ultrasound image demonstrating chronic liver damage ($n = 101/444$; 19.1%). Exclusion criteria for treatment were as follows: neutrophil count <750 cells/μL, platelet count <50,000 cells/μL, hemoglobin level ≤9.0 g/dL, and renal insufficiency (serum creatinine levels >2 mg/dL).

Of 528 patients who received interferon therapy for chronic hepatitis C, 146 were excluded from this study for the following reasons: follow-up <24 weeks after the termination of the interferon therapy ($n = 122$), previously treated for HCC ($n = 22$), or occurrence of HCC during or within 24 weeks after treatment ($n = 2$). Therefore, 382 patients were enrolled for the study and were retrospectively analyzed.

To detect early-stage HCC, ultrasonography, dynamic contrast enhanced computed tomography (CT), dynamic contrast enhanced magnetic resonance imaging (MRI), and/or measurement of tumor markers (including AFP) were performed for all patients at least every 6 months. HCC was diagnosed radiologically as liver tumors displaying arterial hypervascularity and venous or delayed phase washout by dynamic contrast enhanced CT or MRI.

The study protocol was approved by the Ethics Committee at Osaka Red Cross Hospital and performed in compliance with the Helsinki Declaration.

Treatment protocol and definition of responses to treatment

The basic treatment protocol for patients with chronic hepatitis C consisted of 6 mega units of interferon-α-2b 3 times a week or 1.5 μg/kg of pegylated interferon α-2b once a week, combined with ribavirin at an oral dosage of 600–1000 mg/day. Duration of the treatment was 48–72 weeks for those with HCV genotype 1 and serum HCV RNA titer of >5 log IU/mL, and 24 weeks for all other patients.

Patients who were negative for serum HCV RNA for >6 months after completion of interferon therapy were defined as showing an SVR. Patients whose serum ALT levels decreased to the normal range and remained normal for >6 months after the termination of interferon therapy were defined as showing a sustained biochemical response (SBR).

Patients who did not achieve SVR received ursodeoxycholic acid and/or glycyrrhizin containing preparation (Stronger Neo-Minophagen C), when serum ALT levels were higher than the upper limit of normal.

Virological assays

HCV genotype was determined by polymerase chain reaction (PCR) amplification of the core region of the HCV genome using genotype-specific PCR primers [34]. Serum HCV RNA load was evaluated once a month during and 24 weeks after treatment using a PCR assay (Cobas Amplicor HCV Monitor, Roche Molecular Systems, Pleasanton, CA, USA).

Measurement of AFP and calculation of average integration value

AFP was measured in serum samples obtained from each patient at intervals of 1–3 months. The median number of examinations was 15 (range 1–70) in each patient. Serum AFP levels were determined by enzyme-linked immunosorbent assay, which was performed using a commercially available kit (ELISA-AFP, International Reagents, Kobe, Japan). Integration values of AFP and ALT were calculated as described in previous reports [35]. For example, the integration value of AFP was calculated as follows, $(y_0 + y_1) \times x_1/2 + (y_1 + y_2) \times x_2/2 + (y_2 + y_3) \times x_3/2 + (y_3 + y_4) \times x_4/2 + (y_4 + y_5) \times x_5/2 + (y_5 + y_6) \times x_6/2$, i.e., the area of each trapezoid representing an AFP value was measured the sum of the resulting values used to calculate the integration value (Fig. 1). The average integration value was obtained by dividing the integration value by the observation period from initiation of the treatment.

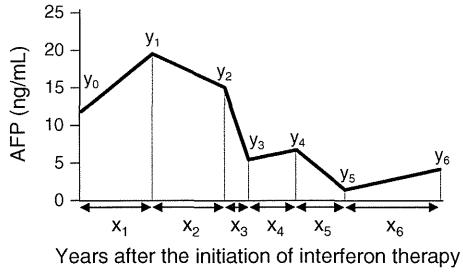

Fig. 1 Example plot of data used for calculation of average integration value of alpha-fetoprotein (AFP)

Statistical analysis

The Kaplan–Meier method was used to estimate the rates of development of HCC in patients after interferon therapy. Log-rank tests were used to evaluate the effects of predictive factors on incidence of HCC. Significance was defined as $P < 0.05$. Multivariate Cox regression analysis using the stepwise method was used to evaluate the association between HCC incidence and patient characteristics, and to estimate hazard ratio (HR) with a 95% confidence interval (CI). A P value of 0.1 was used for variable selection and was regarded as statistically significant. SAS version 9.2 (SAS Institute Inc., Cary, NC, USA) was used for statistical analysis.

Results

Characteristics of patients and incidence of HCC

This study included 382 patients treated for chronic hepatitis C with standard interferon or pegylated interferon in combination with ribavirin. Baseline clinical and virological characteristics of patients included in the study are summarized in Table 1. The median age of the patients at the outset of therapy was 59.0 years (range 18–81 years) and the median follow-up period was 4.1 years (range 0.1–8.4 years). The majority of patients were infected with HCV genotype 1b ($n = 229$; 60%), and median serum HCV RNA load was 6.1 log IU/mL (range 2.3–7.3 log IU/mL). Baseline (before interferon therapy) median serum AFP level was 6.9 ng/mL (range 1.6–478.3 ng/mL).

During follow-up, 23 patients (4.9%) developed HCC. The cumulative incidences of HCC, which was estimated using the Kaplan–Meier method, were 3.1, 6.6, and 13.4% at 3, 5, and 8 years, respectively (Fig. 2).

Predictive factors for incidence of HCC in all patients

Predictive factors for incidence of HCC in all 382 patients were analyzed using log-rank tests (Table 2). Univariate analysis showed that age ≥70 years ($P = 0.040$), non-SVR ($P < 0.0001$), non-SBR ($P = 0.027$), average ALT integration value ≥40 IU/L ($P = 0.001$), baseline AFP ≥10 ng/mL ($P = 0.005$), average AFP integration value ≥10 ng/mL ($P < 0.0001$), and baseline platelet count <150,000 platelets/μL ($P = 0.001$) were all significantly associated with the incidence of HCC. After multivariate analysis, the only variable remaining in the model was non-SVR (HR 8.413, 95% CI 1.068–66.300, $P = 0.043$).

Table 1 Characteristics of 382 patients with hepatitis C treated with interferon therapy in this study

Age (years)	59.0 (18–81)
[a]Males/females	192/190
Observation period (years)	4.1 (0.1–8.4)
[a]IFN + RBV/PEG-IFN + RBV	69/313
HCV genotype 1/2/unclassified	229/57/96
HCV RNA (log IU/mL)	6.1 (2.3–7.3)
White blood cell count (/μL)	4950 (2050–9970)
Hemoglobin (g/dL)	14.0 (10.3–18.8)
Platelet (10^4/μL)	15.0 (5.3–36.4)
AST (IU/L)	56 (17–244)
ALT (IU/L)	67 (16–416)
Bilirubin (mg/dL)	0.8 (0.3–2.4)
AFP (ng/mL)	6.9 (1.6–478.3)

Qualitative variables ([a]) are shown in number, and quantitative variables expressed as median (range)

IFN interferon, *RBV* ribavirin, *PEG-IFN* pegylated interferon, *AST* aspartate aminotransferase, *ALT* alanine aminotransferase, *AFP* alpha-fetoprotein

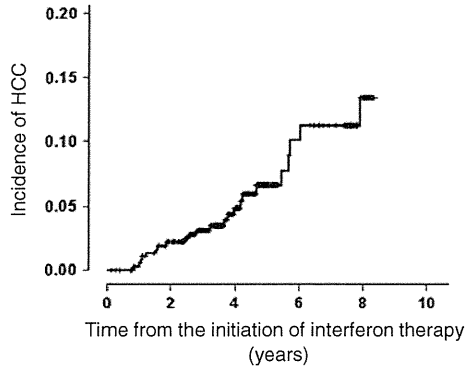

Fig. 2 Incidence of hepatocellular carcinoma (HCC) in 382 patients with hepatitis C who received interferon therapy, estimated using the Kaplan–Meier method

Further, although patients with average AFP integration values ≥10 ng/mL also appeared to have an increased risk of HCC, the difference did not reach statistical significance in the multivariate analysis ($P = 0.050$) (Table 3).

Predictive factors for incidence of HCC in non-SVR patients

Because non-SVR was the only predictive factor across the entire study cohort, to clarify predictive factors for incidence of HCC within this group, the same variables were further analyzed in non-SVR patients alone. By univariate analysis, average AFP integration value ≥10 ng/mL ($P = 0.019$) and baseline platelet count <150,000 ($P = 0.0022$) (Table 2) were again identified as significant predictive factors for incidence of HCC. In addition, male gender was significantly associated with incidence of HCC in non-SVR patients ($P = 0.022$). Multivariate analysis, however, indicated that only two variables were independently associated with incidence of HCC in non-SVR patients: average AFP integration value ≥10 ng/mL (HR 4.039, 95% CI 1.570–10.392, $P = 0.004$), and male gender

Table 2 Univariate analysis of predictive factors for incidence of hepatocellular carcinoma in all 382 and 197 non-SVR patients

Factors	All ($n = 382$)			Non-SVR ($n = 197$)		
	No.	Incidence of HCC ($n = 23$)		No.	Incidence of HCC ($n = 22$)	
		No. (%)	*P* value[a]		No. (%)	*P* value[a]
Age (years)						
<70	359	19 (5)	0.040	182	18 (10)	0.089
≥70	23	4 (17)		15	4 (27)	
Sex						
Female	190	8 (4)	0.125	111	8 (7)	0.022
Male	192	15 (8)		86	14 (16)	
HCV genotype						
1	229	12 (5)	0.452	137	12 (9)	0.796
Non-1	57	1 (2)		10	1 (10)	
Virological response						
SVR	185	1 (1)	<0.0001			
Non-SVR	197	22 (11)				
Biochemical response						
SBR	282	12 (4)	0.027	102	11 (11)	0.857
Non-SBR	86	11 (13)		81	11 (14)	
ALT before IFN therapy						
<40	79	2 (3)	0.274	39	2 (5)	0.319
≥40	301	21 (7)		158	20 (13)	
ALT integration value						
<40	238	6 (3)	0.001	79	5 (6)	0.153
≥40	142	17 (12)		118	17 (14)	
AFP before IFN therapy						
<10	230	7 (3)	0.005	102	7 (7)	0.124
≥10	116	14 (12)		75	13 (17)	
AFP integration value						
<10	258	8 (3)	<0.0001	115	8 (6)	0.019
≥10	63	12 (19)		53	11 (21)	
Platelet before IFN therapy						
<150,000	187	20 (11)	0.001	121	19 (16)	0.022
≥150,000	194	3 (2)		76	3 (4)	

[a] Log-rank test

SVR sustained virological response, *SBR* sustained biochemical response, *ALT* alanine aminotransferase, *IFN* interferon, *AFP* alpha-fetoprotein

Table 3 Multivariate analysis of the predictive factors for incidence of hepatocellular carcinoma in all 382 patients

Factors	Hazard ratio	95% CI	*P* value
Virological response			
SVR	1		
Non-SVR	8.413	1.068–66.300	0.043
AFP integration value			
<10	1		
≥10	2.580	0.999–6.659	0.050

SVR sustained virological response, *IFN* interferon, *AFP* alpha-fetoprotein

Table 4 Multivariate analysis of predictive factors for incidence of hepatocellular carcinoma in 197 non-SVR patients

Factors	Hazard ratio	95% CI	*P* value
AFP integration value			
<10	1		
≥10	4.039	1.570–10.392	0.004
Sex			
Female	1		
Male	3.636	1.383–9.563	0.009

AFP alpha-fetoprotein

(HR 3.636, 95% CI 1.383–9.563, $P = 0.009$) (Table 4). There was no significant difference in other variables including those identified as predictive factors in the entire study population (i.e., age, non-SBR, ALT integration value, AFP before interferon therapy) (Table 2).

AFP integration value as a predictive factor for HCC

Further analysis focused on the AFP integration value as this was the strongest predictive factor for incidence of HCC in non-SVR patients. Of the 382 patients, both baseline and AFP integration values were available for 321. These were divided into four groups: (1) AFP "low–low," (2) AFP "low–high," (3) AFP "high–low," and (4) AFP "high–high," for baseline AFP-average AFP integration values, respectively, where "high" is ≥10 ng/mL and "low" is <10 ng/mL. As shown in Fig. 3a, of the 321 patients, 211 (65.7%) showed baseline AFP levels <10 ng/mL. Of these 211, 207 (98%), were in the AFP low–low group, and only four in the AFP low–high groups. Baseline characteristics, including age, gender, serum HCV-RNA, aspartate aminotransferase (AST), ALT, bilirubin, white blood cell, hemoglobin, platelet, observation periods, and number of times of AFP measurement, were not different between AFP high–low group and high–high group. However, AFP-low group, which is a combination of the low–high and low–low groups, showed significantly lower AST level ($P < 0.00001$), lower ALT level ($P < 0.00001$), higher platelet count ($P < 0.00001$), shorter observation period (P = 0.01448), and fewer number of times of AFP examination ($P = 0.00035$), compared to both AFP high–high and AFP high–low group. Six patients (2.8%) with baseline AFP levels <10 ng/mL developed HCC in the follow-up period and none of these patients were among the four low–high group patients. Even in patients with high baseline AFP levels, incidence of HCC was only 3.9% among the AFP high–low group (2 of 51 patients). In contrast, 20.3% of patients in the AFP high–high group developed HCC during the follow-up period.

The incidence rate of HCC in three patient groups, "AFP-low" (a combination of the "low–high" and "low–low" groups),"high–low," and "high–high", was estimated using the Kaplan–Meier method and compared using log-rank tests (Fig. 3b). The rate of HCC incidence was significantly higher in the AFP high–high group compared to both the AFP high–low group and patients with low baseline AFP levels ($P = 0.009$ and 0.001, respectively). There was no significant difference between patients with low baseline AFP levels and the AFP high–low group. The 7-year incidence rate of HCC was 32.3% in the AFP high–high group, compared to only 6.6% in the AFP high–low group, and 8.1% in all patients with low pre-treatment levels.

Discussion

It is well recognized that the most effective strategy for the prevention of HCC development in patients with chronic hepatitis C is likely to be the complete elimination of the HCV infection accompanied by the resultant normalization of liver function [7, 12, 13, 15, 16, 19]. Indeed, we confirmed here that non-SVR is the most significant predictive factor for incidence of HCC in patients receiving interferon therapy for chronic hepatitis C. However, it should be noted that the risk of HCC, even in non-SVR patients, differs between individuals. In the current study, we identified AFP integration value and male gender as independent risk factors for incidence of HCC in non-SVR patients. The incidence of HCC was significantly reduced in individuals with average AFP integration values < 10 ng/mL after interferon therapy, which suggests that the decrease of AFP by interferon therapy lowers the risk of developing HCC. Indeed, even where patients had high baseline AFP levels, incidence of HCC was reduced when the AFP integration value decreased after interferon therapy. Thus, our current findings identify AFP integration value as a useful predictive marker of HCC development in non-SVR patients.

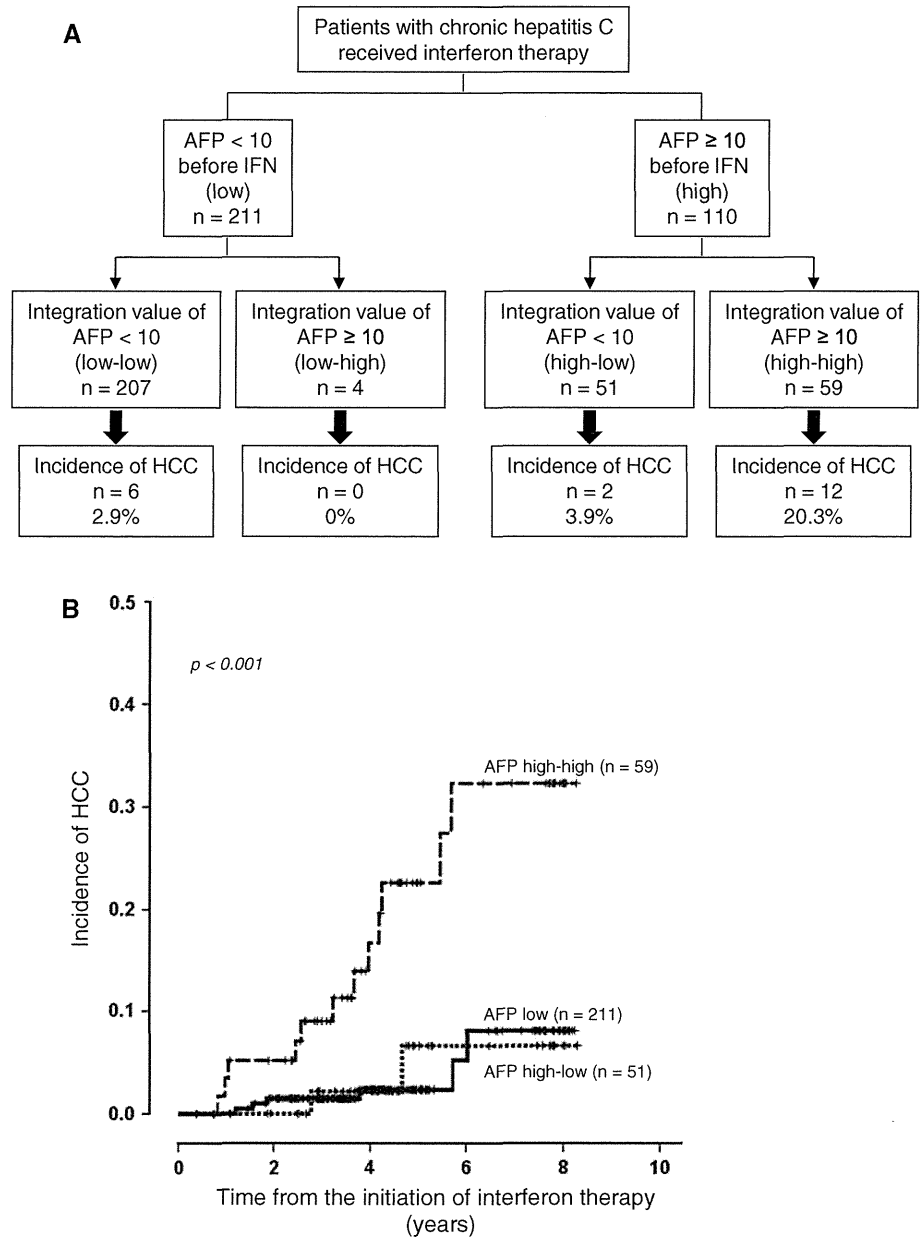

Fig. 3 AFP integration value as a predictive factor for HCC. **a** *Flow diagram* showing the number of patients (*n*) classified by baseline alpha-fetoprotein (AFP) levels before interferon (IFN) therapy and average AFP integration value, and the incidence of hepatocellular carcinoma (HCC) of each group. **b** Kaplan–Meier estimates of the incidence of HCC. *Solid line* AFP-low group (AFP levels before interferon therapy <10 ng/mL); *dotted line* AFP high–low group (baseline AFP levels ≥10 ng/mL, average AFP integration value <10 ng/mL); *dashed line* AFP high–high group (both baseline and average AFP integration values ≥10 ng/mL)

Data from several previous studies suggest that the continuous normalization of alanine aminotransferase (ALT) levels by interferon therapy can reduce the risk of HCC development [36–39]. In addition, one recent study suggested that the ALT integration value is a predictive factor for HCC [35]. In contrast to published data (22), our multivariate analysis did not identify the ALT integration value as a significant predictive factor for HCC incidence, although it was identified as significant by univariate analysis in all 382 patients. Since the previous study did not evaluate AFP levels as a factor for prediction of HCC [35], our results indicate that the AFP integration value is superior to that of ALT as a predictive factor for incidence of HCC. We do not know the reason for this result, but it is speculated that significance of AFP as a marker of hepatic regeneration resulted in the more accurate prediction of hepatocarcinogenesis by integration value of AFP than that of ALT.

As AFP is a diagnostic marker for the existence of HCC, high integration value of AFP in the present study might be a result of HCC development. However, we concluded that the high AFP integration values in patients who developed HCC were not caused by a result of existence of HCC, because of the following two reasons. First, the last AFP values before detection of HCC were not the highest level in the follow-up periods in 19 of 23 patients who developed

HCC, suggesting that the AFP was not produced by the developing HCC in these patients. Second, to exclude the influence of the remaining four patients whose last AFP levels were the highest in the follow-up periods, we analyzed the same statistical analysis by using average AFP integration values excluded the last two examinations of AFP before the detection of HCC. The results of the analysis also showed average integration value of AFP as a significant predictive factor for incidence of HCC.

Male gender was also identified as an independent risk factor for HCC in non-SVR patients in this study. Several reports have shown that men are at a higher risk of developing HCC than women [6, 10, 33, 40, 41]. The male gender also appears to be a risk factor for more severe disease and a greater risk of developing cirrhosis in chronic hepatitis C [42]. Although the association of male gender with the risk of HCC is as yet unexplained, hormonal or genetic factors may lead to increased risk for HCC and cirrhosis in men as previously discussed [10].

In conclusion, a decrease in the AFP integration value predicts reduced incidence of HCC in patients with hepatitis C receiving interferon therapy. Further prospective studies with a larger number of patients are required to validate the significance of these findings.

Acknowledgments This work was supported by Grants-in-aid for Scientific Research from the Ministry of Education, Culture, Sports, Science and Technology, and the Ministry of Health, Labor and Welfare of Japan.

Conflict of interest The authors declare that they have no conflict of interest.

References

1. Bruix J, Barrera JM, Calvet X, Ercilla G, Costa J, Sanchez-Tapias JM, Ventura M, Vall M, Bruguera M, Bru C, et al. Prevalence of antibodies to hepatitis C virus in Spanish patients with hepatocellular carcinoma and hepatic cirrhosis. Lancet. 1989;2:1004–6.
2. Colombo M, Kuo G, Choo QL, Donato MF, Del Ninno E, Tommasini MA, Dioguardi N, Houghton M. Prevalence of antibodies to hepatitis C virus in Italian patients with hepatocellular carcinoma. Lancet. 1989;2:1006–8.
3. Hasan F, Jeffers LJ, De Medina M, Reddy KR, Parker T, Schiff ER, Houghton M, Choo QL, Kuo G. Hepatitis C-associated hepatocellular carcinoma. Hepatology. 1990;12:589–91.
4. Ikeda K, Saitoh S, Koida I, Arase Y, Tsubota A, Chayama K, Kumada H, Kawanishi M. A multivariate analysis of risk factors for hepatocellular carcinogenesis: a prospective observation of 795 patients with viral and alcoholic cirrhosis. Hepatology. 1993;18:47–53.
5. Tsukuma H, Hiyama T, Tanaka S, Nakao M, Yabuuchi T, Kitamura T, Nakanishi K, Fujimoto I, Inoue A, Yamazaki H, et al. Risk factors for hepatocellular carcinoma among patients with chronic liver disease. N Engl J Med. 1993;328:1797–801.
6. Fattovich G, Stroffolini T, Zagni I, Donato F. Hepatocellular carcinoma in cirrhosis: incidence and risk factors. Gastroenterology. 2004;127:S35–50.
7. Ikeda K, Marusawa H, Osaki Y, Nakamura T, Kitajima N, Yamashita Y, Kudo M, Sato T, Chiba T. Antibody to hepatitis B core antigen and risk for hepatitis C-related hepatocellular carcinoma: a prospective study. Ann Intern Med. 2007;146:649–56.
8. Liang TJ, Heller T. Pathogenesis of hepatitis C-associated hepatocellular carcinoma. Gastroenterology. 2004;127:S62–71.
9. Yoshida H, Shiratori Y, Moriyama M, Arakawa Y, Ide T, Sata M, Inoue O, Yano M, Tanaka M, Fujiyama S, Nishiguchi S, Kuroki T, Imazeki F, Yokosuka O, Kinoyama S, Yamada G, Omata M. Interferon therapy reduces the risk for hepatocellular carcinoma: national surveillance program of cirrhotic and noncirrhotic patients with chronic hepatitis C in Japan. IHIT Study Group. Inhibition of hepatocarcinogenesis by interferon therapy. Ann Intern Med. 1999;131:174–81.
10. Heathcote EJ. Prevention of hepatitis C virus-related hepatocellular carcinoma. Gastroenterology. 2004;127:S294–302.
11. Lok AS, Seeff LB, Morgan TR, di Bisceglie AM, Sterling RK, Curto TM, Everson GT, Lindsay KL, Lee WM, Bonkovsky HL, Dienstag JL, Ghany MG, Morishima C, Goodman ZD. Incidence of hepatocellular carcinoma and associated risk factors in hepatitis C-related advanced liver disease. Gastroenterology. 2009; 136:138–48.
12. Effect of interferon-alpha on progression of cirrhosis to hepatocellular carcinoma: a retrospective cohort study. International Interferon-alpha Hepatocellular Carcinoma Study Group. Lancet. 1998;351:1535–9.
13. Camma C, Giunta M, Andreone P, Craxi A. Interferon and prevention of hepatocellular carcinoma in viral cirrhosis: an evidence-based approach. J Hepatol. 2001;34:593–602.
14. Di Bisceglie AM, Shiffman ML, Everson GT, Lindsay KL, Everhart JE, Wright EC, Lee WM, Lok AS, Bonkovsky HL, Morgan TR, Ghany MG, Morishima C, Snow KK, Dienstag JL. Prolonged therapy of advanced chronic hepatitis C with low-dose peginterferon. N Engl J Med. 2008;359:2429–41.
15. Fattovich G, Giustina G, Degos F, Diodati G, Tremolada F, Nevens F, Almasio P, Solinas A, Brouwer JT, Thomas H, Realdi G, Corrocher R, Schalm SW. Effectiveness of interferon alfa on incidence of hepatocellular carcinoma, decompensation in cirrhosis type C. European Concerted Action on Viral Hepatitis (EUROHEP). J Hepatol. 1997;27:201–5.
16. Hayashi K, Kumada T, Nakano S, Takeda I, Kiriyama S, Sone Y, Toyoda H, Shimizu H, Honda T. Incidence of hepatocellular carcinoma in chronic hepatitis C after interferon therapy. Hepatogastroenterology. 2002;49:508–12.
17. Lok AS, Everhart JE, Wright EC, Di Bisceglie AM, Kim HY, Sterling RK, Everson GT, Lindsay KL, Lee WM, Bonkovsky HL, Dienstag JL, Ghany MG, Morishima C, Morgan TR. Maintenance peginterferon therapy and other factors associated with hepatocellular carcinoma in patients with advanced hepatitis C. Gastroenterology. 2011;140:840–9.
18. Nishiguchi S, Kuroki T, Nakatani S, Morimoto H, Takeda T, Nakajima S, Shiomi S, Seki S, Kobayashi K, Otani S. Randomised trial of effects of interferon-alpha on incidence of hepatocellular carcinoma in chronic active hepatitis C with cirrhosis. Lancet. 1995;346:1051–5.
19. Okanoue T, Itoh Y, Minami M, Sakamoto S, Yasui K, Sakamoto M, Nishioji K, Murakami Y, Kashima K. Interferon therapy lowers the rate of progression to hepatocellular carcinoma in chronic hepatitis C but not significantly in an advanced stage: a retrospective study in 1148 patients. Viral Hepatitis Therapy Study Group. J Hepatol. 1999;30:653–9.
20. Izuno K, Fujiyama S, Yamasaki K, Sato M, Sato T. Early detection of hepatocellular carcinoma associated with cirrhosis by combined assay of des-gamma-carboxy prothrombin and alpha-fetoprotein: a prospective study. Hepatogastroenterology. 1995;42:387–93.

21. Trevisani F, D'Intino PE, Morselli-Labate AM, Mazzella G, Accogli E, Caraceni P, Domenicali M, De Notariis S, Roda E, Bernardi M. Serum alpha-fetoprotein for diagnosis of hepatocellular carcinoma in patients with chronic liver disease: influence of HBsAg and anti-HCV status. J Hepatol. 2001;34:570–5.
22. Zoli M, Magalotti D, Bianchi G, Gueli C, Marchesini G, Pisi E. Efficacy of a surveillance program for early detection of hepatocellular carcinoma. Cancer. 1996;78:977–85.
23. Alpert E, Feller ER. Alpha-fetoprotein (AFP) in benign liver disease. Evidence that normal liver regeneration does not induce AFP synthesis. Gastroenterology. 1978;74:856–8.
24. Bloomer JR, Waldmann TA, McIntire KR, Klatskin G. Alpha-fetoprotein in noneoplastic hepatic disorders. JAMA. 1975;233:38–41.
25. Ruoslahti E, Seppala M. Normal and increased alpha-fetoprotein in neoplastic and non-neoplastic liver disease. Lancet. 1972;2:278–9.
26. Sakurai T, Marusawa H, Satomura S, Nabeshima M, Uemoto S, Tanaka K, Chiba T. *Lens culinaris* agglutinin-A-reactive alpha-fetoprotein as a marker for liver atrophy in fulminant hepatic failure. Hepatol Res. 2003;26:98–105.
27. Taketa K. Alpha-fetoprotein: reevaluation in hepatology. Hepatology. 1990;12:1420–32.
28. Di Bisceglie AM, Sterling RK, Chung RT, Everhart JE, Dienstag JL, Bonkovsky HL, Wright EC, Everson GT, Lindsay KL, Lok AS, Lee WM, Morgan TR, Ghany MG, Gretch DR. Serum alpha-fetoprotein levels in patients with advanced hepatitis C: results from the HALT-C Trial. J Hepatol. 2005;43:434–41.
29. Tateyama M, Yatsuhashi H, Taura N, Motoyoshi Y, Nagaoka S, Yanagi K, Abiru S, Yano K, Komori A, Migita K, Nakamura M, Nagahama H, Sasaki Y, Miyakawa Y, Ishibashi H. Alpha-fetoprotein above normal levels as a risk factor for the development of hepatocellular carcinoma in patients infected with hepatitis C virus. J Gastroenterol. 2011;46:92–100.
30. Murashima S, Tanaka M, Haramaki M, Yutani S, Nakashima Y, Harada K, Ide T, Kumashiro R, Sata M. A decrease in AFP level related to administration of interferon in patients with chronic hepatitis C and a high level of AFP. Dig Dis Sci. 2006;51:808–12.
31. Tamura Y, Yamagiwa S, Aoki Y, Kurita S, Suda T, Ohkoshi S, Nomoto M, Aoyagi Y. Serum alpha-fetoprotein levels during and after interferon therapy and the development of hepatocellular carcinoma in patients with chronic hepatitis C. Dig Dis Sci. 2009;54:2530–7.
32. Arase Y, Ikeda K, Suzuki F, Suzuki Y, Kobayashi M, Akuta N, Hosaka T, Sezaki H, Yatsuji H, Kawamura Y, Kumada H. Prolonged-interferon therapy reduces hepatocarcinogenesis in aged-patients with chronic hepatitis C. J Med Virol. 2007;79:1095–102.
33. Asahina Y, Tsuchiya K, Tamaki N, Hirayama I, Tanaka T, Sato M, Yasui Y, Hosokawa T, Ueda K, Kuzuya T, Nakanishi H, Itakura J, Takahashi Y, Kurosaki M, Enomoto N, Izumi N. Effect of aging on risk for hepatocellular carcinoma in chronic hepatitis C virus infection. Hepatology. 2010;52:518–27.
34. Ohno O, Mizokami M, Wu RR, Saleh MG, Ohba K, Orito E, Mukaide M, Williams R, Lau JY. New hepatitis C virus (HCV) genotyping system that allows for identification of HCV genotypes 1a, 1b, 2a, 2b, 3a, 3b, 4, 5a, and 6a. J Clin Microbiol. 1997;35:201–7.
35. Kumada T, Toyoda H, Kiriyama S, Sone Y, Tanikawa M, Hisanaga Y, Kanamori A, Atsumi H, Takagi M, Nakano S, Arakawa T, Fujimori M. Incidence of hepatocellular carcinoma in hepatitis C carriers with normal alanine aminotransferase levels. J Hepatol. 2009;50:729–35.
36. Arase Y, Ikeda K, Suzuki F, Suzuki Y, Kobayashi M, Akuta N, Hosaka T, Sezaki H, Yatsuji H, Kawamura Y, Kumada H. Interferon-induced prolonged biochemical response reduces hepatocarcinogenesis in hepatitis C virus infection. J Med Virol. 2007;79:1485–90.
37. Kasahara A, Hayashi N, Mochizuki K, Takayanagi M, Yoshioka K, Kakumu S, Iijima A, Urushihara A, Kiyosawa K, Okuda M, Hino K, Okita K. Risk factors for hepatocellular carcinoma, its incidence after interferon treatment in patients with chronic hepatitis C. Osaka Liver Disease Study Group. Hepatology. 1998;27:1394–402.
38. Kurokawa M, Hiramatsu N, Oze T, Mochizuki K, Yakushijin T, Kurashige N, Inoue Y, Igura T, Imanaka K, Yamada A, Oshita M, Hagiwara H, Mita E, Ito T, Inui Y, Hijioka T, Yoshihara H, Inoue A, Imai Y, Kato M, Kiso S, Kanto T, Takehara T, Kasahara A, Hayashi N. Effect of interferon alpha-2b plus ribavirin therapy on incidence of hepatocellular carcinoma in patients with chronic hepatitis. Hepatol Res. 2009;39:432–8.
39. Suzuki K, Ohkoshi S, Yano M, Ichida T, Takimoto M, Naitoh A, Mori S, Hata K, Igarashi K, Hara H, Ohta H, Soga K, Watanabe T, Kamimura T, Aoyagi Y. Sustained biochemical remission after interferon treatment may closely be related to the end of treatment biochemical response and associated with a lower incidence of hepatocarcinogenesis. Liver Int. 2003;23:143–7.
40. Kurosaki M, Hosokawa T, Matsunaga K, Hirayama I, Tanaka T, Sato M, Yasui Y, Tamaki N, Ueda K, Tsuchiya K, Kuzuya T, Nakanishi H, Itakura J, Takahashi Y, Asahina Y, Enomoto N, Izumi N. Hepatic steatosis in chronic hepatitis C is a significant risk factor for developing hepatocellular carcinoma independent of age, sex, obesity, fibrosis stage and response to interferon therapy. Hepatol Res. 2010;40:870–7.
41. Takahashi H, Mizuta T, Eguchi Y, Kawaguchi Y, Kuwashiro T, Oeda S, Isoda H, Oza N, Iwane S, Izumi K, Anzai K, Ozaki I, Fujimoto K. Post-challenge hyperglycemia is a significant risk factor for the development of hepatocellular carcinoma in patients with chronic hepatitis C. J Gastroenterol. 2011;46:790–8.
42. Forns X, Ampurdanes S, Sanchez-Tapias JM, Guilera M, Sans M, Sanchez-Fueyo A, Quinto L, Joya P, Bruguera M, Rodes J. Long-term follow-up of chronic hepatitis C in patients diagnosed at a tertiary-care center. J Hepatol. 2001;35:265–71.